Computer Simulation of Conformational Transitions in an Idealized Polymer Model

J. H. Weiner* and M. R. Pear

Division of Engineering and Department of Physics, Brown University, Providence, Rhode Island 02912. *Received October 4, 1976*

ABSTRACT: A highly idealized model of a long-chain molecule with internal energy barriers and under applied tension is studied both analytically and by computer simulation. Equilibrium properties are computed exactly on the basis of equilibrium statistical mechanics. In the fully extended and stretched state the model exhibits a transition in behavior, over a narrow range of temperature, from that appropriate to a harmonic crystal at low temperature levels to that characteristic of a polymer at higher temperature levels. The computer simulation procedure uses the Langevin equation and yields equilibrium values which agree well with the theoretical equation of state. The observed barrier crossing rates under equilibrium conditions agree reasonably well with a simple rate theory formulation although there are some systematic deviations. Computer simulation tests at constant cooling rate show "freezing" of the length at a nonequilibrium value at sufficiently high rates of cooling. Comparison is made with the theory of Vol'kenshtein and Ptitsyn; there is qualitative agreement but substantial quantitative discrepancies.

I. Introduction

In this paper we present results of a computer simulation study of the dynamics of an idealized long-chain molecule. This molecule is visualized as part of a polymeric solid network under stress so that in addition to intramolecular forces there is an applied force at the ends of the molecule which is regarded as transmitted by the rest of the network. We are particularly interested in the effects of internal rotation barriers in a polymer on its time-dependent behavior.

We have attempted here, as the first step in our investigation of this process, to keep our model as simple as possible while still retaining the principal physical features of a long-chain molecule with internal rotational barriers. The one-dimensional model employed is described in section II.

Because of the simplicity of the model employed, it is possible to develop a complete treatment of its equilibrium properties by use of equilibrium statistical mechanics. This is discussed in section III both for the case of short chains for which ensembles of fixed length and fixed stress give different results and for the thermodynamic limit of chains of infinite length. The case of stretched long-chain molecules has, of course, been extensively studied previously by various authors. A good summary may be found in Vol'kenshtein.[1] There is substantial overlap between these previous results and the present work. However, we present them here for completeness and to provide a basis for the computer simulation studies of its nonequilibrium properties. In addition, we also study in this section the behavior of the molecule in its fully extended and stretched state. Although this state is rarely of direct physical concern, it is of some interest to note that the model in this state exhibits a transition over a narrow range of temperature from behavior characteristic of a harmonic crystal to behavior characteristic of polymeric solids.

Computer simulation of the model, described in section IV, is based on the use of the classical Langevin equation in order to produce the characteristics of the chain when immersed in a heat bath at elevated temperature. The work is therefore similar in spirit to that of Simon and Zimm,[2] although directed toward a different class of phenomena and employing a somewhat different numerical procedure.[3] After verification that the numerical procedure adequately simulates conditions of thermal equilibrium by examining the velocity distribution and by comparing the simulated equilibrium properties with the theoretical results of section III, attention is turned to the simulation of nonequilibrium properties of the system. The first type of nonequilibrium test involves a step change in temperature. A short induction period is found to be necessary before the system reacts to the step increase and contracts. This induction period appears to depend upon chain length, becoming longer with increasing chain length. It is expected that the nonequilibrium properties of the model are closely related to the barrier-crossing rates during equilibrium conditions. The computer program includes provisions for determining barrier crossing rates both in the direction which serves to increase chain length and in the direction which decreases chain length. It is found that these barrier-crossing rates agree fairly well with the simplest rate theory describing such a process, one which neglects complexities such as cooperative effects, or the strength of heat bath interactions. However, there are some systematic deviations which require further study.

The model we have studied here treats only intramolecular barriers and omits any intermolecular interactions. It is therefore too simplified at this stage to permit comparison with theories of the glass transition such as that of Gibbs–DiMarzio[4] which includes both flex energy (intramolecular) and hole energy (intermolecular). However, it is possible to compare it with the relaxation theory of Vol'kenshtein and Ptitsyn[5] for the glass transition which assumes for simplicity a single relaxation process. Computer simulation runs were made in which a constant cooling rate was imposed on the model and these results are compared with the Vol'kenshtein and Ptitsyn theory in section V.

Conclusions and directions for further work are presented in section VI.

II. Model Description

Our goal in the design of the model of a long-chain molecule to be studied is to obtain a high degree of simplicity while including the feature of the existence of internal barriers to bond rotation. As a starting point, consider a long-chain molecule such as the polyethylene molecule $(CH_2)_n$, Figure 1a, in which only the carbon atoms are shown and in which each C–C bond can rotate, i.e., the bond C_1C_2 can rotate about C_0C_1 as an axis, C_2C_3 about C_1C_2 as an axis, etc., while all the bond lengths C_0C_1, C_1C_2, . . . and the valence angles $C_0C_1C_2$, $C_1C_2C_3$, . . . remain constant. Because of the presence of side groups, there are energy barriers to rotation, typically of the order of magnitude of 3–5 kcal/mol, as shown in Figure 1b.

As a first step in simplification, this three-dimensional situation may be idealized by regarding the configuration as restricted to the plane, as in Figure 1c, with rotation now taking place about an axis through each carbon atom perpendicular to the plane of the molecule. The energy barriers to rotation about these axes are still regarded as of the form

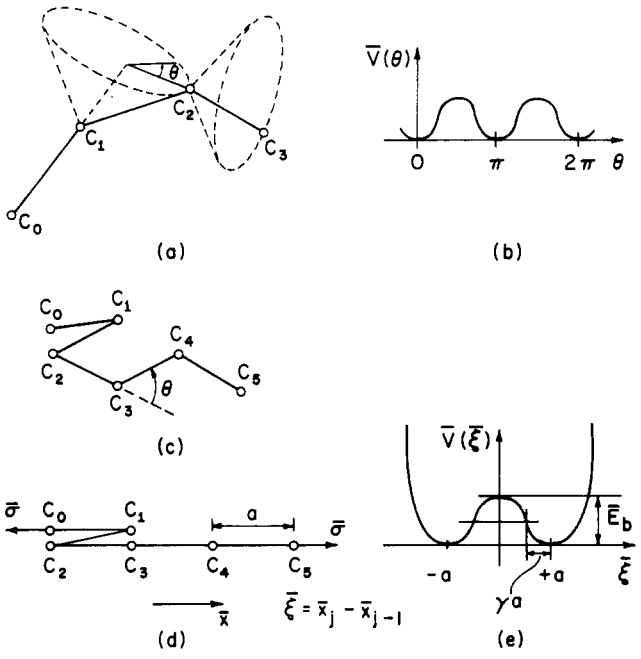

Figure 1. Model description: (a) three-dimensional picture of a portion of the backbone of a long-chain molecule showing rotations about the bonds; (b) rotational potential barriers due to side groups; (c) two-dimensional idealization; (d) projection to one-dimension; (e) interaction potential for the one-dimensional model (eq 1).

shown in Figure 1b. As a final step, to simplify matters still further, this two-dimensional model is, in effect, projected onto a single dimension as shown in Figure 1d. Here, the atoms are constrained to move on a straight line in the $\bar{x}$ direction and the position of the j'th atom at time t is denoted[17] by $\bar{x}_j(t)$. Nearest neighbor atoms interact with a two-body potential $\bar{V}(\bar{\xi})$, where $\bar{\xi} = \bar{x}_j - \bar{x}_{j-1}$, as shown in Figure 1e. At first glance it may seem strange that the potential $\bar{V}(\bar{\xi})$ permits $\bar{x}_j - \bar{x}_{j-1}$ to change sign since that appears to allow an atom to pass through its neighbor. However, it must be emphasized that our model is regarded as a conceptual projection from two dimensions down to one, and the passing of $\bar{x}_j - \bar{x}_{j-1}$ from $+a$ to $-a$ is the analogue of the rotation through 180° about an atom of Figure 1c. The energy barrier at $V(0)$ in Figure 1e therefore corresponds to the rotational barrier presented by $V(\theta)$ at $\theta = \pi/2, 3\pi/2$ in Figure 1b. For simplicity we have taken $\bar{V}(\bar{\xi})$ as a piece-wise quadratic function which is continuous, with continuous derivatives, and defined as (Figure 1e)

$$\begin{aligned} \bar{V}(\bar{\xi}) &= \tfrac{1}{2}k_w a^2\gamma - \frac{k_w\gamma}{2(1-\gamma)}\bar{\xi}^2, \text{ for } |\bar{\xi}| \le a(1-\gamma) \\ \bar{V}(\bar{\xi}) &= \tfrac{1}{2}k_w(a - |\bar{\xi}|)^2, \text{ for } |\bar{\xi}| \ge a(1-\gamma) \end{aligned} \tag{1}$$

where a is the unstretched link length, k_w is the spring constant for small changes of link length, and $a\gamma$ is the distance from well bottom to change in potential curvature. For this potential, the barrier height $\bar{E}_b$ is given by

$$\bar{E}_b = \tfrac{1}{2}k_w a^2\gamma \tag{2}$$

We regard the long-chain molecule as part of a network under stress and therefore it is assumed that the end atoms of the chain, corresponding to $j = 0$ and $j = N$, are subjected to a constant force $\bar{\sigma}$ in the $\bar{x}$ direction, with positive $\bar{\sigma}$ corresponding to tension. In what follows we sometimes refer loosely to the force $\bar{\sigma}$ as the "applied stress".

It is now convenient to introduce the dimensionless variables which will be employed throughout the remainder of the paper:

$$x_j = \bar{x}_j/a,\ \xi = \bar{\xi}/a,\ \sigma = \bar{\sigma}/(k_w a),\ V = \bar{V}/(k_w a^2),$$
$$E_b = \bar{E}_b/k_w a^2 = \gamma/2,\ T = k_B\bar{T}/(k_w a^2)$$

where, in addition to previously defined quantities, $\bar{T}$ denotes temperature and k_B is Boltzman's constant.

III. Equilibrium Properties

(a) Exact Evaluation. Because of the simplicity of the model it is possible to compute its equilibrium properties explicitly by use of equilibrium statistical mechanics. In what follows it is convenient to fix $x_0 = 0$ so that the force σ need be applied only to the N'th atom and so that l, the end-to-end length of the chain in any configuration, is simply $l = x_N$. We consider two different thermal equilibrium ensembles: (1) l fixed, σ fluctuates; and (2) σ fixed, l fluctuates. The appropriate configurational partition function for each of these ensembles respectively is:

$$Z_l(l,T) = \int_{-\infty}^{\infty} dx_1 \cdots \int_{-\infty}^{\infty} dx_{N-1} \times \exp\left\{-\beta \sum_{j=0}^{N-1} V(x_{j+1} - x_j)\right\} \tag{3}$$

$$Z_\sigma(\sigma,T) = \int_{-\infty}^{\infty} dx_1 \cdots \int_{-\infty}^{\infty} dx_N \times \exp\left\{-\beta\left(\sum_{j=0}^{N-1} V(x_{j+1} - x_j) - \sigma x_N\right)\right\} \tag{4}$$

where $\beta = T^{-1}$. Note that the parameter $l = x_N$ appears in the expression for $Z_l(l,T)$ as argument of $V(x_{j+1} - x_j)$ for $j = N - 1$. It may be verified by direct computation that

$$\langle\sigma\rangle(l,T) = \left\langle \frac{\partial V}{\partial x_N} \right\rangle (l,T) = -\frac{1}{\beta}\frac{\partial \ln}{\partial l} Z_l(l,T) \tag{5}$$

$$\langle l\rangle(\sigma,T) = \frac{1}{\beta}\frac{\partial \ln}{\partial \sigma} Z_\sigma(\sigma,T) \tag{6}$$

where $\langle \ldots \rangle$ denotes the phase average of the indicated quantity. For systems with small finite N, such as those studied in the next section by computer simulation, the functions $\langle\sigma\rangle(l,T)$ and $\langle l\rangle(\sigma,T)$ are not equivalent.[6] We defer this question until later in this section and confine attention first to the case of the thermodynamic limit ($N \to \infty$) in which the relative fluctuations vanish so that we may write $\langle\sigma\rangle = \sigma$, $\langle l\rangle = l$. Under these conditions the relations $\sigma(l,T)$ and $l(\sigma,T)$ given by eq 5 and 6 are both equivalent to a single equation of state, $f(\sigma,l,T) = 0$. They may also be put in the context of macroscopic thermodynamics by noting that

$$\begin{aligned} F(l,T) &= -\frac{1}{\beta}\ln Z_l(l,T) \\ G(\sigma,T) &= -\frac{1}{\beta}\ln Z_\sigma(\sigma,T) \end{aligned} \tag{7}$$

where $F = U - TS$ and $G = U - TS - \sigma l$ are respectively the Helmholtz and Gibbs free energy functions and that, from macroscopic thermodynamics,

$$\sigma = \left.\frac{\partial F}{\partial l}\right|_T; \quad l = -\left.\frac{\partial G}{\partial \sigma}\right|_T \tag{8}$$

Of the two ensembles, it is more convenient to utilize that in which σ is fixed and to evaluate $l(\sigma,T)$ by use of eq 4 and 6.

We start by utilizing the orthogonal coordinate transformation[7]

$$\xi_j = x_{j+1} - x_j, \quad j = 0, 1, \ldots, N-1 \tag{9}$$

so that

$$l = x_N - x_0 = \sum_{j=0}^{N-1} \xi_j \tag{10}$$

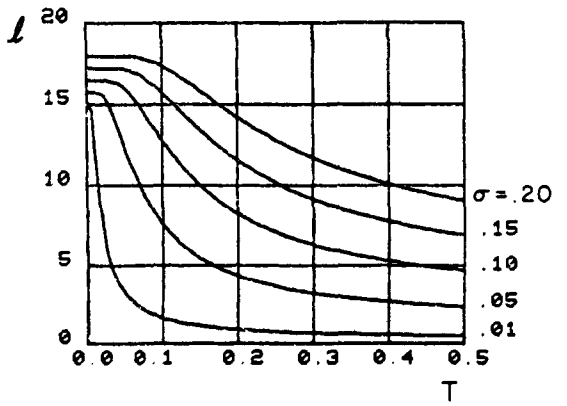

Figure 2. Graph of $l(\sigma,T)$ as defined in eq 18; $N = 15$ and $\gamma = 0.5$.

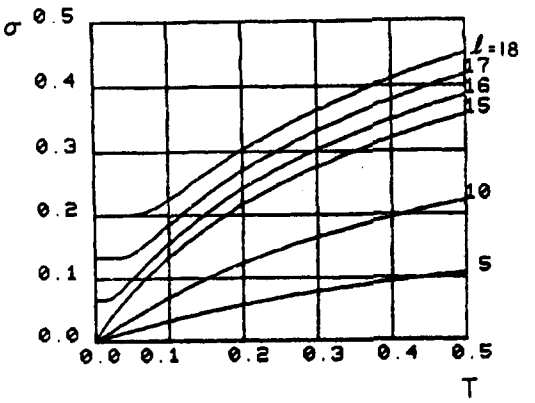

Figure 3. Functional dependence of $\sigma(l,T)$ as obtained by numerical inversion of eq 18; $N = 15$ and $\gamma = 0.5$.

Then $Z_\sigma(\sigma,T)$ can be written as the product

$$Z_\sigma(\sigma,T) = (Z_1(\sigma,T))^N \tag{11}$$

where

$$Z_1(\sigma,T) = \int_{-\infty}^{\infty} d\xi \exp\{-\beta(V(\xi) - \sigma\xi)\} \tag{12}$$

It follows from eq 6, 11, and 12 that

$$l(\sigma,T) = N\langle\xi\rangle \tag{13}$$

where

$$\langle\xi\rangle = \frac{1}{\beta}\frac{\ln Z_1}{\partial\sigma} = Z_1^{-1}\int_{-\infty}^{\infty} d\xi\, \xi \exp\{-\beta(V(\xi) - \sigma\xi)\} \tag{14}$$

For the potential function $V(\xi)$ given in eq 1 it is found that

$$Z_1 = I_+ + I_b + I_- \tag{15}$$

where

$$I_\pm = \left(\frac{\pi\gamma}{2\beta}\right)^{1/2} e^{(\beta/2\gamma)(\sigma^2 \pm 2\sigma)} \operatorname{erfc}\left(-\left(\frac{\beta}{2}\right)^{1/2}(\gamma \pm \sigma)\right)$$

$$I_b = \left(\frac{\pi}{2\beta\alpha}\right)^{1/2} e^{(-\beta/2)\gamma + (\sigma^2/\alpha)}\left[\phi\left(\left(\frac{\beta}{2\alpha}\right)^{1/2}(\sigma + \gamma)\right) - \phi\left(\left(\frac{\beta}{2\alpha}\right)^{1/2}(\sigma - \gamma)\right)\right] \tag{16}$$

$$\alpha = \gamma/(1 - \gamma)$$

and

$$\phi(y) = \frac{2}{(\pi)^{1/2}}\int_0^y e^{x^2} dx \tag{17}$$

is Dawson's integral.[8] Then, by application of eq 13 and 14, it is found that

$$l(\sigma,T) = NZ_1^{-1}\left[(\sigma + 1)I_+ - \frac{\sigma}{\alpha}I_b + (\sigma - 1)I_- + \frac{2}{\beta\gamma}e^{-\beta\gamma^2/2}\sinh(\beta\sigma(1 - \gamma))\right] \tag{18}$$

The evaluation of eq 18 for selected parameter values is shown in Figure 2. The functional dependence of $\sigma(l,T)$ may be obtained by numerical inversion of $l(\sigma,T)$; it is shown in Figure 3. The following features of the equilibrium behavior of the model may be observed:

(1) If the equilibrium length is fixed at a value corresponding to a nonfully extended chain, i.e., $l < N$, then the σ vs. T dependence has the monotonically increasing appearance expected for a long-chain molecule.

(2) Although the behavior of a long-chain molecule in its fully extended and stretched states is rarely of direct physical concern, it is nevertheless of some interest to explore the behavior of this idealized model in this regime. It is seen (Figure 3) that for values of $l > N$, there is a range of temperature, starting at $T = 0$, for which the stress σ required to maintain the length l is virtually independent of T. This is characteristic of the behavior of a harmonic crystal. There is then a transition over a narrow range of temperature to the monotonically increasing σ vs. T dependence characteristic of a polymer.

(3) This transition in behavior is also seen in the dependence of l on T for fixed σ (Figure 2). Here the harmonic crystalline behavior is evidenced by the absence of thermal expansion at low-temperature levels, with a transition at higher temperatures to the contraction upon temperature increases characteristic of polymers.

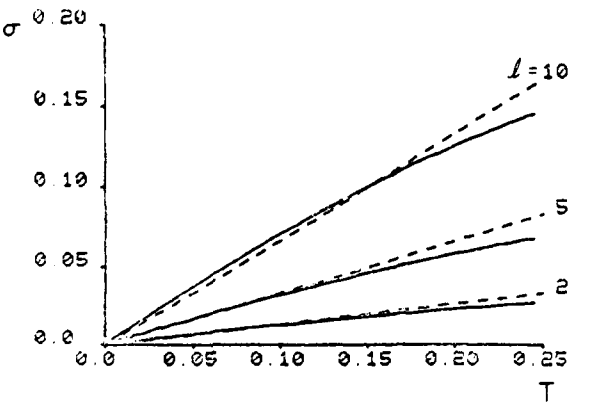

Figure 4. Comparison of combinatorial calculation (- - -) with numerical inversion of eq 18 (—); $N = 15$ and $\gamma = 0.5$.

(b) Approximate Evaluations. At low temperature and stress levels it is clear that the values of $\xi_j = x_{j+1} - x_j$ will be confined to the neighborhoods of the potential minima of $V(\xi)$, that is $\xi_j = \pm 1$ with large probability. Under these conditions the present model reduces to that considered by Kubo[9] and the stress–temperature relation may be computed by the combinatorial procedure outlined by him with the result, in the present notation, that for a prescribed integer-valued length l,

$$\sigma = (l/N)T \tag{19}$$

This relation is shown in Figure 4 together with the exact relation obtained from the numerical inversion of the $l(\sigma,T)$ relation of eq 18. The agreement is seen to be good up until values of $T \sim 0.15$. This is reasonable since for higher temperature levels, the assumption that $\xi_j = \pm 1$ with high probability is no longer valid. The combinatorial result also uses Stirling's formula which requires that $l/N \ll 1$; this explains

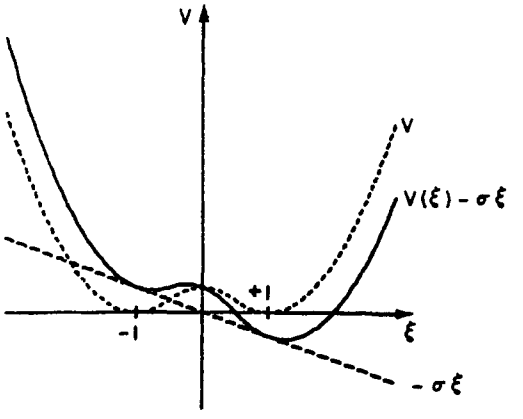

Figure 5. Effect of applied stress on potential wells of Figure 1e. The sum of $V(\xi)$ and $-\sigma\xi$ gives the effective potential well.

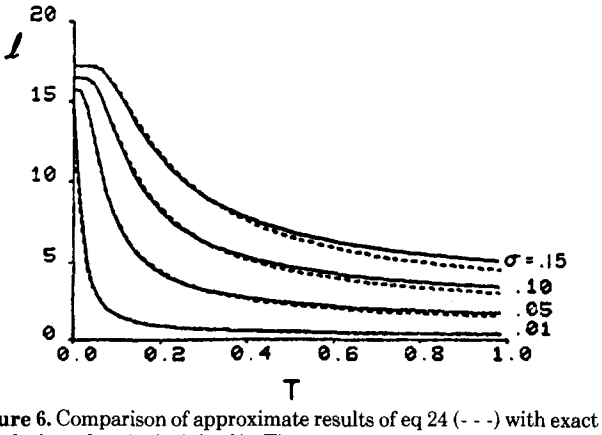

Figure 6. Comparison of approximate results of eq 24 (- - -) with exact calculation of eq 18 (—) for $l(\sigma,T)$.

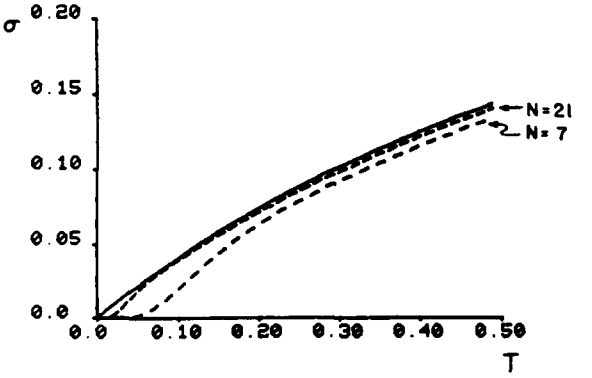

Figure 7. Comparison of numerical inversion (—) of eq 18 with Laplace transform inversions (- - -) for $N = 7$ and $N = 21$; $l/N = \frac{3}{7}$ for the three curves.

the increasing discrepancy between it and the exact result for increasing l.

We may go beyond the combinatorial calculation which assumes that $\xi_j = \pm 1$ with high probability by noting that for low-temperature levels the values of ξ will be confined to the neighborhoods of the potential minima, but that the values of these minima and their locations are affected by the applied stress σ (Figure 5). For the piece-wise quadratic potential $V(\xi)$ defined in eq 1 and with an applied stress $\sigma < \gamma$, the locations of the minima $\xi_0^{\pm}$ of the function $V(\xi) - \sigma\xi$ are

$$\xi_0^{\pm} = \pm 1 + \sigma \tag{20}$$

and the values of these minima are

$$V(\xi_0^{\pm}) - \sigma\xi_0^{\pm} = \mp\sigma - \sigma^2/2 \tag{21}$$

For $\beta \gg 1$, the major contributions to the integrals in the expressions for $Z_1(\sigma,T)$ and $\langle\xi\rangle$ (eq 12 and 14) come from the neighborhoods of $\xi_0^{\pm}$ in which the function $V(\xi) - \sigma\xi$ is small. These integrals therefore are readily approximated to give the results

$$Z_1(\sigma,T) = e^{\beta\sigma^2/2}(e^{\beta\sigma} + e^{-\beta\sigma}) \tag{22}$$

$$\langle\xi\rangle \cong \frac{(-1+\sigma)e^{-\beta(\sigma-(\sigma^2/2))} + (1+\sigma)e^{\beta(\sigma+(\sigma^2/2))}}{e^{-\beta(\sigma-(\sigma^2/2))} + e^{\beta(\sigma+(\sigma^2/2))}} \tag{23}$$

If it is assumed further that $\sigma \ll 1$,

$$\langle\xi\rangle \simeq \tanh(\beta\sigma) + \sigma \tag{24}$$

The approximate result of eq 24 is compared with the exact result of eq 18 in Figure 6; it is seen to agree quite well. Finally, we note that if in addition to the inequalities $\beta \gg 1$, $\sigma \ll 1$, we require that $\beta\sigma \ll 1$ then eq 24 reduces to $\beta\sigma = \langle\xi\rangle$ which is equivalent, by use of eq 13, to the combinatorial result of eq 19 but without the requirement that l be integer valued.

(c) Behavior for Small N. From the definitions of $Z_l(l,T)$ and $Z_\sigma(\sigma,T)$, eq 3 and 4, it is seen that

$$Z_\sigma(\sigma,T) = \int_{-\infty}^{\infty} dl'\, e^{+\beta\sigma l'} Z_l(l',T) = \mathcal{L}\{Z_l(l,T)\} \tag{25}$$

where $\mathcal{L}\{\ldots\}$ denotes the two-sided Laplace transform with $-\beta\sigma$ playing the role of transform parameter and therefore

$$Z_l(l,T) = \mathcal{L}^{-1}\{Z_\sigma(\sigma,T)\} = \frac{-\beta}{2\pi i}\int_{-i\infty}^{i\infty} Z(\sigma',T)e^{-\beta\sigma' l}\, d\sigma' \tag{26}$$

where $\mathcal{L}^{-1}\{\ldots\}$ is the inverse transform as determined by the usual inversion integral.[10] While the latter is too difficult to evaluate for the exact $Z_\sigma(\sigma,T)$ (eq 11 and 15–17), the computation is readily carried through with the use of the approximate $Z_\sigma(\sigma,T)$ (eq 11 and 22). The result is (Appendix)

(eq 11 and 22). The result is (Appendix)

$$Z_l(l,T) \simeq \sqrt{\beta/2\pi N}\sum_{r=0}^{N}\binom{N}{r} e^{-\beta(N-2r-l)^2/2N} \tag{27}$$

Equation 5 is then employed to give

$$\langle\sigma\rangle(l,T) \simeq \frac{1}{N}\frac{\sum_{j=0}^{N}\binom{N}{j}(2j-N+l)e^{-\beta(N-2j+l)^2/N}}{\sum_{r=0}^{N}\binom{N}{r}e^{-\beta(N-2r+l)^2/2N}} \tag{28}$$

The result of eq 28 is compared in Figure 7 with that obtained by the numerical inversion of the $l(\sigma,T)$ relation that follows from eq 13 and 24.

It is seen that the result of eq 28, valid for small N, is below that following from eq 24 and converges to it for large N as expected.

In addition to the overlap with previous work on stretched molecules (Vol'kenshtein[1]) already noted, the result of the present section may be compared with that of Wehner and Baeriswyl[11] which came to our attention after this work was completed. They are also concerned with the classical statistical mechanics of the double-well potential, motivated by the problem of structural phase transitions in crystalline solids. As has been customary in that field, they study a potential containing a quadratic and a quartic term. The piece-wise quadratic potential utilized here permits a simpler analytic treatment of the problem without altering the essential physical behavior.

IV. Computer Simulation

(a) Langevin Formulation. In order to study the time-dependent aspects of the model, we assume that the random

interactions of the atoms of the long-chain molecule with its environment at temperature T may be represented by use of the Langevin equation. The defining equations of the model then take the form

$$\ddot{x}_j = -\frac{\partial V}{\partial x_j}(x_j - x_{j-1}) - \frac{\partial V}{\partial x_j}(x_{j+1} - x_j) - \eta\dot{x}_j + F_j$$
$$j = 1, \ldots, N-1 \tag{29}$$
$$\ddot{x}_N = \sigma - \frac{\partial V}{\partial x_N}(x_N - x_{N-1}) - \eta\dot{x}_N + F_N$$
$$x_0(t) \equiv 0$$

Superposed dots denote differentiation with respect to dimensionless time t, defined in terms of dimensional time $\bar{t}$ by the relation

$$t = (k_w/m)^{1/2}\bar{t} \tag{30}$$

where m is the mass of the atoms of the chain and k_w is the spring constant for small displacements as defined in eq 1. The terms $-\eta\dot{x}_j + F_j$ represent, within the classical Langevin equation framework, the force on the j'th atom due to the other molecules of the network regarded as a heat bath at temperature T. This force is composed therefore of two parts: the friction force[18] $-\eta\dot{x}_j$ and the random fluctuating part $F_j(t)$. These two terms are related as seen in the following description of the statistical characteristics of $F_j(t)$: Let Δt be a time interval sufficiently short such that during it the position and velocity of the atom change very little but $F_j(t)$ suffers many fluctuations. Let

$$B_j(\Delta t) = \int_t^{t+\Delta t} F_j(\tau)\,d\tau \tag{31}$$

be the impulse (assumed independent of t) imparted to the j'th atom during this time interval by the fluctuating force F_j. Then the probability of occurrence of different values of $B_j(\Delta t)$ is governed by the distribution function[12]

$$\rho(B_j(\Delta t)) = \frac{1}{(2\pi q\Delta t)^{1/2}} \exp\left(-\frac{|B_j(\Delta t)|^2}{2q\Delta t}\right) \tag{32}$$

where, in the nondimensional notation here employed,

$$q = 2\eta T \tag{33}$$

This choice of $\rho(B_j(\Delta t))$ (which is independent of j) ensures that the distribution of each atom's position and velocity will, after a sufficiently long period, assume the characteristics of thermal equilibrium at temperature T.

In formulating the finite-difference equivalents of eq 29, it should be emphasized that we are not seeking a numerical procedure for computing an approximation to the solutions $x_j(t)$ which will converge to the true solutions as the numerical time step $\delta t \to 0$. This is not possible since the velocity $v_j(t) = \dot{x}_j(t)$ has the property of being everywhere nondifferentiable.[13] Rather, the time interval Δt, described prior to eq 31, is regarded as the smallest of physical interest and the computer simulation calculates only statistical information about the atoms' positions and velocities for time periods long with respect to Δt.

In order to produce a random fluctuating force with the characteristics given by eq 25–27, the following procedure has been found convenient.[3] Let the finite-difference time step used in the computation, δt, be taken as a small fraction of Δt; $F_j(t)$ is taken as constant in each successive time interval δt with the value

$$F_j = (-1)^{R_j}((q/\delta t)^{1/2} \tag{34}$$

where R_j is an odd or even integer with equal probability, selected independently for each atom. Then it follows from the central limit theorem that the probability distribution function for $B(\Delta t)$ will approach the required Gaussian form of eq 26 as $\delta t/\Delta t \to 0$.

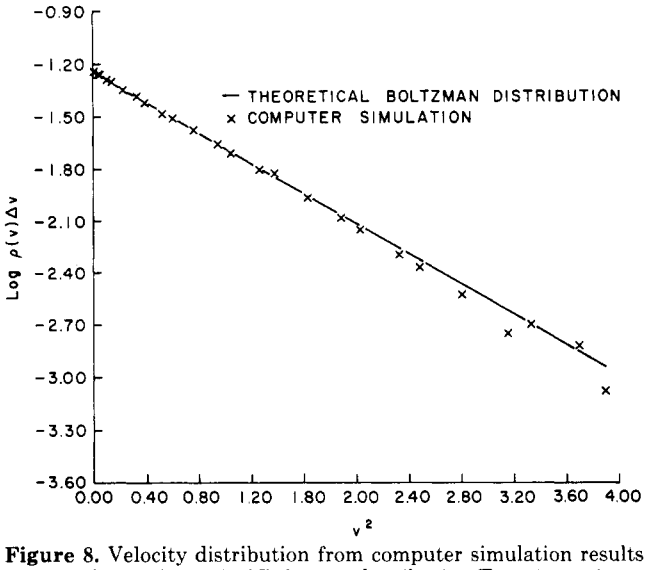

Figure 8. Velocity distribution from computer simulation results compared with theoretical Boltzman distribution $T = 0.5$, $\sigma = 0.1$, $\gamma = 0.5$, $N = 15$.

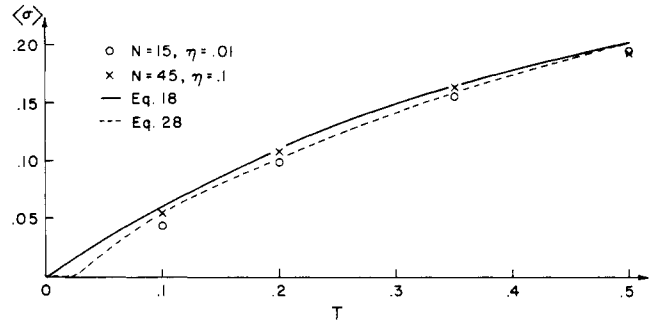

Figure 9. Comparison of computer simulation results with theory, $l/N = 9/15$ and $\gamma = 0.5$ for all curves except that based upon eq 28 which does not depend upon γ.

With F_j defined as in eq 34, eq 29 was solved numerically by use of the Runge–Kutta fourth-order process.[14] The procedure required approximately 5×10^{-3} s of CPU time per atom and per unit t on the IBM 360-67.

(b) Numerical Results. (i) Thermal Equilibrium Characteristics. In order to check that the numerical procedure was adequately simulating conditions of thermal equilibrium in the model, computer runs were made at constant temperature and stress and a sorting routine on the atom velocities v_j was employed to determine the fraction of time the atoms spent in different velocity ranges. A typical result is shown in Figure 8 where the numerical results are compared with the theoretical Boltzman distribution, and it is seen that the agreement is good.

(ii) Equilibrium $l(\sigma,T)$ Relationship. As a second check on the numerical procedure, l and T were maintained fixed and the corresponding time average of σ was determined by computer simulation. The results of such a computation are compared in Figure 9 with the theoretical result of eq 18 (exact for $N \to \infty$) and the approximate result, eq 28, valid for finite N. Both theoretical results are quite close, but the computer simulation results appear to agree better with the latter as would be expected.

(iii) Step Change in Temperature. In Figures 10a and 10b, the atom trajectories are shown for the case in which the

stress σ is held fixed and the temperature, after being held constant at T_1 for an initial period, is raised discontinuously to $T_2 > T_1$ and then again held fixed. The decrease in length, characteristic of rubber elasticity, upon rise in temperature under constant load is noted. It is also seen that there is a period of delay after the change of temperature is imposed before the system reacts. It appears that the computational method of imposing the temperature change (by suddenly changing the random force magnitude introduced in eq 33 and 34) is equivalent to suddenly plunging the system into a heat bath at the new temperature. The system then requires some time to attain this new temperature. If the new ambient temperature were imposed only at the end atoms, it would be expected from the macroscopic theory of transient heat conduction that such a delay time would be proportional to N^2, which appears to be approximately the case for the results of Figures 10a and 10b. However, in this computation the new temperature is simultaneously imposed on each atom, so that the cause of a length-dependent delay period is not clear.

(iv) Barrier-Crossing Rates. In this particular computer simulation study we were concerned with the question of the possible role of cooperative effects on the barrier-crossing rates as occasioned, for example, by the fact that some types of jumps require the motion of large portions of the chain.[15] To this end we simulated two different chain lengths and treated two types of end conditions, one with fixed σ and one with fixed l.

We consider first the case in which σ is fixed. Let $\langle n_\pm \rangle$ be the average occupation of the wells centered at $\xi_0^\pm$ as defined in eq 20. Since

$$\begin{gathered}\langle n_+\rangle(1+\sigma) + \langle n_-\rangle(-1+\sigma) = \langle l\rangle \\ \langle n_+\rangle + \langle n_-\rangle = N\end{gathered} \tag{35}$$

it follows that

$$\langle n_\pm\rangle = \frac{N(1 \mp \sigma) \pm \langle l\rangle}{2} \tag{36}$$

At equilibrium

$$\langle n_+\rangle f_{+-} = \langle n_-\rangle f_{-+} \tag{37}$$

where f_{+-} is the fractional rate of barrier crossings from the well at ξ_0^+ to the well at ξ_0^-, and similarly for f_{-+}.

The computer-simulation program includes provision for determining the total rate of barrier crossings which take place in each direction. By the use of eq 36 and 37, using the observed value of $\langle l\rangle$, it is then possible to compute the fractional rates f_{+-} and f_{-+} at various temperature levels.

Simulation studies were also made (run 2) for the same chain parameters with the length fixed at each temperature T at a value given by $l(\sigma,T)$ for the same value of σ as in the previous calculations. The rates f_{+-}, f_{-+} were computed by an analogous procedure to that described in eq 35–37.

The results of these two calculations (with $N = 15$, runs 1 and 2) are shown in Figures 11 and 12. A third computation with $N = 60$ and with fixed σ (run 3) was also made and the results are shown in Figure 13. It is seen that the rates obey an Arrhenius relation of the form

$$f = \frac{\omega}{2\pi} e^{-\beta U} \tag{38}$$

On the basis of the simplest rate theory, neglecting such complexities as cooperative effects, etc., we would expect that, in the dimensionless units employed,

$$\begin{gathered}\omega_{+-}{}^{\mathrm{th}} = \omega_{-+}{}^{\mathrm{th}} = (k_w/m)^{1/2} = 1 \\ U_{+-}{}^{\mathrm{th}} = E_b + \sigma, \quad U_{-+}{}^{\mathrm{th}} = E_b - \sigma, \\ U_{av}{}^{\mathrm{th}} = \tfrac{1}{2}((U_{+-}{}^{\mathrm{th}} + U_{-+}{}^{\mathrm{th}}) = E_b\end{gathered} \tag{39}$$

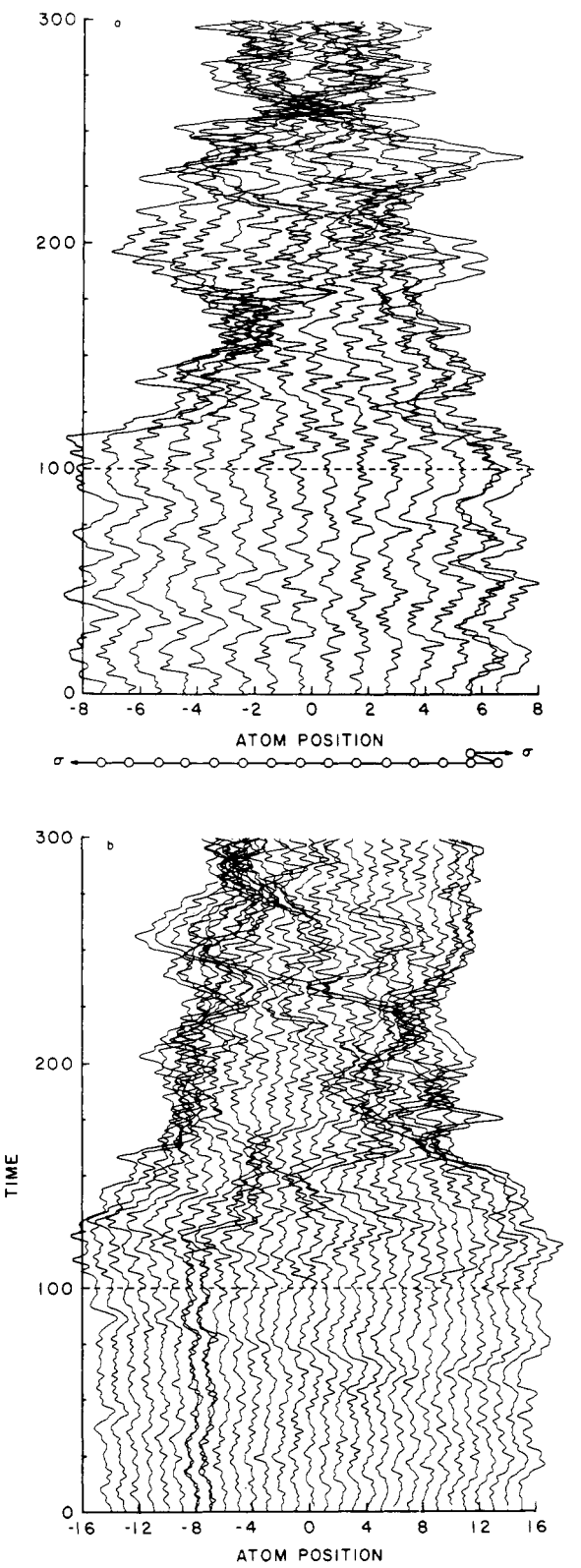

Figure 10. Effect of discontinuous temperature change on model. Figures show atom trajectories as a function of time referred to center of mass as origin. Temperature changed at $t = 100$ from $T_1 = 0.0375$ to $T_2 = 0.15$; (a) $N = 15$. Shown also is model configuration at $t = 0$; (b) $N = 31$.

The parameters determined by least-squares fit from the simulation results are listed in Table I and compared there with the theoretical results of eq 39. There appears to be little difference between the fixed σ and fixed l condition and the computer simulation results appear to agree reasonably well with the simple theory of eq 39, although the observed fre-

Table I
Barrier-Crossing Rates

Run No.	Figure No.	γ	N	Fixed parameter	t_f[a]	ω_{+-}	ω_{-+}	U_{+-}	U_{-+}	U_{av}
1	11	0.25	15	σ	1200	1.351	1.451	0.170	0.095	0.133
2	12	0.25	15	l	1200–2200	1.395	1.451	0.183	0.101	0.142
3	13	0.25	60	σ	1200	1.213	1.722	0.158	0.131	0.145
Eq 39		0.25				1.0	1.0	0.175	0.075	0.125

[a] Length of computations in dimensionless units.

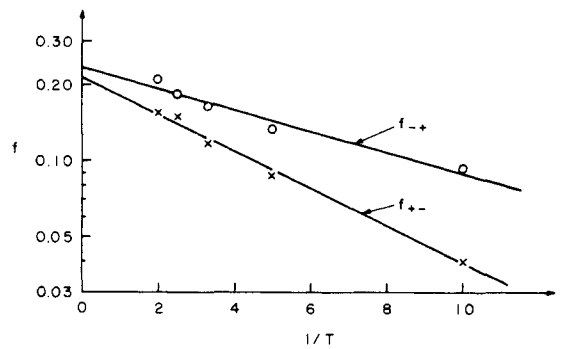

Figure 11. Barrier crossing rates for $N = 15$, $\sigma = 0.05$, and $\gamma = 0.25$ (corresponding to $E_b = 0.125$). Lines in Figures 11–13 are least-squares fits to data points for f_{+-} and f_{-+} with resulting parameters listed in Table I.

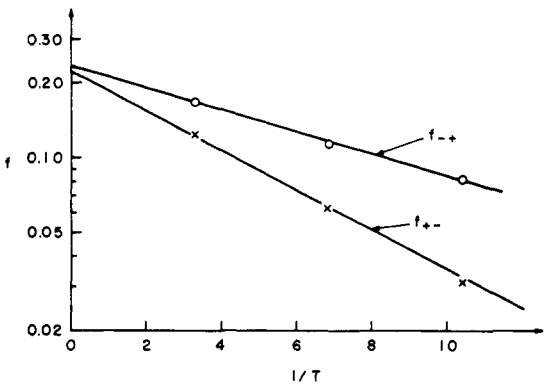

Figure 12. Barrier crossing rates for $N = 15$, $\gamma = 0.25$ ($E_b = 0.125$), and length l held constant. Length l was fixed at each temperature but was adjusted at each temperature level to maintain $\langle\sigma\rangle \simeq 0.5$.

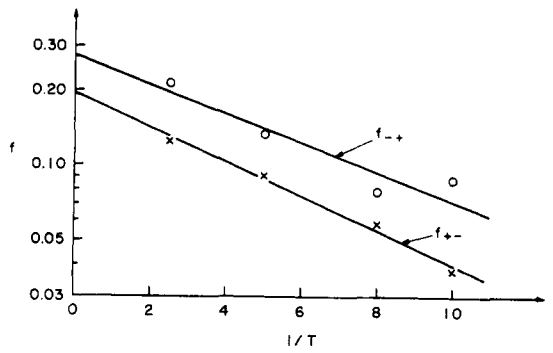

Figure 13. Barrier-crossing rates for $N = 60$, $\gamma = 0.25$ ($E_b = 0.125$), and $\sigma = 0.05$.

quency factors are consistently higher than that theory indicates and the results for the longer chain depart from that theory more than do those for the short chain. Whether this difference is real or is an artifact of the computer simulation procedure will require further study.

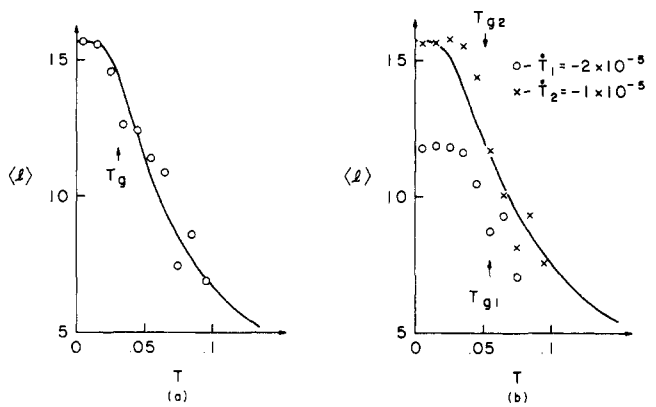

Figure 14. Length dependence on temperature during steady cooling. Data points are observed averaged (as described in text) lengths during cooling; the curve represents equilibrium values as given by eq 18. The value of T_g shown is that predicted by the VP theory, eq 40; $N = 15$, $\sigma = 0.05$: (a) $\gamma = 0.25$ ($E_b = 0.125$), cooling rate $\dot{T} = -2 \times 10^{-5}$; (b) $\gamma = 0.5$ ($E_b = 0.25$), (○) $\dot{T} = -2 \times 10^{-5}$, (×) $\dot{T} = -1 \times 10^{-5}$. T_{g1} corresponds to $\dot{T} = -2 \times 10^{-5}$; T_{g2} corresponds to $\dot{T} = -1 \times 10^{-5}$.

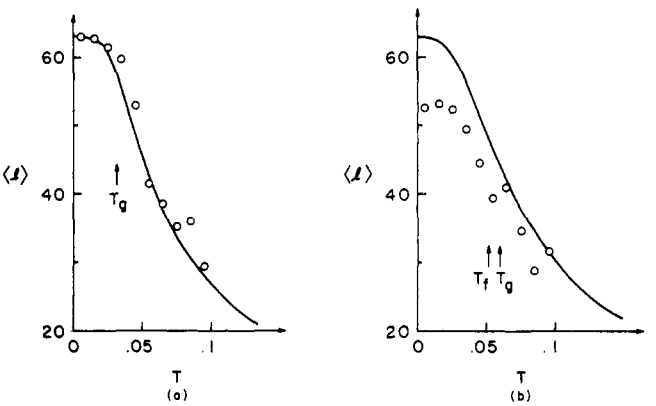

Figure 15. Length dependence on temperature during steady cooling as in Figure 14; $N = 60$, $\sigma = 0.05$, $\dot{T} = -2 \times 10^{-5}$: (a) $\gamma = 0.25$ ($E_b = 0.125$); (b) $\gamma = 0.5$ ($E_b = 0.25$). The values of T_g and T_f shown are those predicted by the VP theory, eq 40 and 41.

(v) Steady Cooling. Previously the results of a discontinuous change in temperature were discussed. Computations were also made with the imposed temperature decreased at a steady rate. The results of these computations are shown in Figures 14 and 15. Each data point is obtained by averaging the observed length over a time interval in which the temperature decreased by 0.01.

In Figure 14, results are shown for a chain with $N = 15$. Figure 14a shows results for $\gamma = 0.25$, corresponding to a barrier height $E_b = 0.125$, with a cooling rate $\dot{T} = -2 \times 10^{-5}$. As can be seen, the observed length follows the theoretical equilibrium curve very well.

In Figure 14b, the results of a similar computation are shown, the only change being a doubling of the barrier height ($\gamma = 0.5, E_b = 0.25$). At low temperature levels ($T \sim 0.04$) the length "freezes" at a value well below that of the equilibrium curve. Below this temperature level barrier crossing ceases for the time scale of the computation. In the region where the observed length is changing, there is a noticeable lag between the data points corresponding to steady cooling and the equilibrium curve.

These calculations were repeated with $N = 60$ (Figure 15). There is no great change in the results, although the scatter of the observed length is reduced. Also, in Figure 15b, the temperature at which the final length is reached is lower than for the shorter chain.

Another run is presented in Figure 14b for a cooling rate of $\dot{T} = -1 \times 10^{-5}$, one-half the rate of the other computations. In this computation, the observed length does not "freeze" at as low a value as at the high rate but reaches the fully extended length. However, this length is arrived at a higher temperature level than predicted by the equilibrium curve. This behavior may be understood on the basis of a barrier-crossing rate which is the same for each run at a corresponding temperature. This results cooling and allows the chain configuration to adjust more closely to the equilibrium values.

Vol'kenshtein and Ptitsyn[5] (VP) have presented a relaxation theory for the glass transition. This theory, which assumes for simplicity a single relaxation process, is based upon a first-order rate equation which results in the following relation for T_g, the vitrification temperature, during cooling:

$$\frac{\nu e^{-U/T_g}}{|\dot{T}|} = \frac{U}{T_g^2} \tag{40}$$

where $\nu = \omega/2\pi$ is the frequency factor, U is the barrier height, and T is the rate of temperature change. In order to evaluate eq 40 for the present computer simulation experiments, the parameters ν and U were taken from the barrier-crossing data as listed in Table I. Since these parameters refer only to the case $\gamma = 0.25$, they are extended to the case $\gamma = 0.5$ by doubling activation energies and leaving frequency factors unchanged. Since it was found that T_g as predicted by eq 40 is relatively insensitive to small changes in these parameters, this procedure appears reasonable. The predicted transition temperatures are indicated in Figures 14 and 15 by arrows. It can be seen that, in general, the value of T_g predicted by VP is greater than the temperature at which the computer simulation results exhibit a noticeable change in behavior which might be regarded as a transition. However, the VP result does indicate a change in T_g for the different barrier heights which is consistent, at least qualitatively, with the observed data. Also, the predicted dependence of T_g on the cooling rate is also qualitatively in accord with the simulation results.

The theory of VP also predicts that, during steady cooling, the configuration of the system at a temperature T near T_g corresponds to the equilibrium configuration at some higher temperature. This is in qualitative agreement with the computer simulation results, but the observed lag is much larger than that predicted. The VP theory also predicts that the final configuration will correspond to the equilibrium structure at the temperature

$$T_f = T_g - 0.58\frac{T_g^2}{U} \tag{41}$$

The temperature T_f is shown in Figure 15b and is higher than observed in the computer simulation results.

In general, it was found that there was qualitative agreement between the VP theory and the computer simulation results as regards (a) the dependence of the transition temperature on the barrier height, (b) the effect of the cooling rate on the transition temperature, and (c) the lag between the observed length and the equilibrium length. Further work is needed to determine whether the substantial quantitative discrepancies reflect shortcomings in the VP theory, the computer simulation procedures, or both.

VI. Conclusions

The principal purpose of the present paper was to determine if computer simulation techniques utilizing the Langevin equation could provide insight and serve as a useful tool for the study of the dynamic mechanical properties of polymers. Our general conclusion is that they can and that further studies along these lines, involving both the idealized model treated here and also more realistic models, are indicated.

The model treated in this paper is, of course, far from an accurate description of real polymers. Nevertheless, it does incorporate some of their important features such as chain flexibility, internal energy barriers, and the effect of applied stress. It can, therefore, serve as a model system for testing our grasp of an appropriate theoretical framework for dealing with these questions. By computer simulation of the model we can acquire "experimental data" against which existing theories can be checked. This can provide a more stringent test than comparison with experiments on real systems, for with a model system there are no unknown parameters, such as barrier heights, to be adjusted to obtain fits between theory and experiment.

Some of the specific results obtained from this initial study are as follows:

(a) Equilibrium properties for this highly idealized model may be computed exactly on the basis of classical equilibrium statistical mechanics.

(b) Although the fully extended and stretched state of a polymer molecule is rarely of direct physical concern, the equilibrium properties of this model under these conditions show an interesting transition in behavior, over a narrow range of temperature, from that appropriate to a harmonic crystal at low-temperature levels to that characteristic of a polymer at higher temperature levels.

(c) The computer simulation procedure using the Langevin equation yields equilibrium properties for the model which agree well with the theoretical equation of state.

(d) The computer program contains provision for determination of the barrier-crossing rates in both directions, those which increase and those which decrease the length of the chain. These rates agree reasonably well with the simplest rate-theory estimates although there are some systematic deviations. In particular, the observed frequency factors are about 40% higher than those predicted by the simple theory.

(e) Persistence effects in barrier crossings are observed as in Figure 10 where it is noted that the crossing of one barrier is frequently followed by the crossing of many successive barriers.

(f) With the model under an applied tensile stress, a step increase in temperature results in the expected decrease in length. However, a short induction period is observed before the model begins to react to the change in imposed temperature. This induction period appears to be molecular length dependent.

(g) Computer simulation tests were made corresponding to cooling of the model at different rates while under constant stress. At slow rates the observed length followed the equilibrium curve but at high rates, the length departed from this curve and became "frozen" at a nonequilibrium value. These results were compared with the theory of Vol'kenshtein and Ptitsyn[5] (VP). While qualitative agreement was noted there were substantial quantitative discrepancies.

As noted, the present work was regarded as a preliminary step to gain experience with the model and the computer simulation technique. Numerous questions present themselves for further investigation. Among them are the following:

(i) Helfand[15] has presented an extensive study of the rates of conformational changes in polymers utilizing the concepts of Kramers' rate theory[16] for a single particle in a viscous medium and of localized modes in a harmonic chain. He has dealt primarily with the high friction limit ($\eta \gg 1$ in our notation) whereas we have here treated the case of $\eta \ll 1$. It would be of interest to study the behavior of our model in the former regime, to evaluate Helfand's theory for this model, and to compare the results of computer simulation with the theoretical predictions.

(ii) Further work involving cooling runs is indicated. This would serve to make more precise the degree of departure of the computer results from the VP theory and should help determine what modifications in that theory are needed to secure better agreement.

(iii) While still retaining its present simple one-dimensional form, the model may be modified to include simulated interactions with other chains of a network. This would then permit comparison with the Gibbs–DiMarzio[4] theory of the glass transition and also provide a basis for the study of time-dependent processes in polymers due to chain–chain interactions.

(iv) The model may be extended to be fully three dimensional. The insights provided by the one-dimensional model should prove useful in suggesting the types of calculations to be performed on the more complex model.

Acknowledgments. This work has been supported by the American Gas Association (Grant No. BR 122-1) and by the National Science Foundation (Grant No. ENG 75-16069).

Appendix

Starting with eq 36 and the approximate partition function of eq 22, we get

$$Z_l(l,T) = \frac{-\beta}{2\pi i}\int_{-i\infty}^{i\infty} e^{N\beta\sigma^2/2}(e^{\beta\sigma} + e^{-\beta\sigma})^N e^{-\beta\sigma l}\,d\sigma \tag{A1}$$

Since integral is along imaginary axis, the variable change $\sigma = ix$ can be applied to give

$$Z_l(l,T) = \frac{\beta}{2\pi}\int_{-\infty}^{\infty} e^{-N\beta x^2/2}(e^{i\beta x} + e^{-i\beta x})^N e^{-i\beta x l}\,dx \tag{A2}$$

Then, expanding the integrand according to the binomial theorem,

$$Z_l(l,T) = \frac{\beta}{2\pi}\int_{-\infty}^{\infty} e^{-N\beta x^2/2}\sum_{r=0}^{N}\binom{N}{r} \times (e^{i\beta x})^{N-r}(e^{-i\beta x})^r e^{-i\beta x l}\,dx \tag{A3}$$

and reversing the order of the summation and integration,

$$Z_l(l,T) = \frac{\beta}{2\pi}\sum_{r=0}^{N}\binom{N}{r}\int_{-\infty}^{\infty}\exp\left(-\frac{N\beta}{2}x^2 + i\beta x(N-2r+l)\right)dx \tag{A4}$$

These integrals are easily evaluated by completing the square of the exponent in the integrand so that

$$\int_{-\infty}^{\infty}\exp(\ldots)\,dx = \left(\frac{2\pi}{N\beta}\right)^{1/2}\exp\left(\frac{-\beta(N-2r-l)^2}{2N}\right) \tag{A5}$$

Therefore,

$$Z_l(l,T) = \left(\frac{\beta}{2\pi N}\right)^{1/2}\sum_{r=0}^{N}\binom{N}{r}e^{-\beta(N-2r-l)^2/2N} \tag{A6}$$

Applying eq 5 to the above expression gives the relation for $\langle\sigma\rangle(l,T)$ as in eq 28.

References and Notes

(1) M. V. Vol'kenshtein, "Configurational Statistics of Polymeric Chains", Interscience, New York, N.Y., 1963, Chapter 8 (English Translation).
(2) E. M. Simon and B. H. Zimm, *J. Stat. Phys.*, **1**, 41 (1969).
(3) J. H. Weiner and R. E. Forman, *Phys. Rev. B*, **10**, 315 (1974).
(4) J. H. Gibbs and E. A. DiMarzio, *J. Chem. Phys.*, **28**, 373 (1958).
(5) M. V. Vol'kenshtein and O. B. Ptitsyn, *Sov. Phys.-Tech. Phys. (Engl. Transl.)*, **1**, 2138 (1957).
(6) T. L. Hill, "Thermodynamics of Small Systems", Part I, W. A. Benjamin, New York, N.Y., 1963, p 154.
(7) H. Takahasi, *Proc. Phys.-Math. Soc. Jpn.*, **24**, 60 (1942).
(8) M. Abramowitz and I. Stegun, Ed., *Natl. Bur. Stand., Appl. Math. Ser.*, **No. 55**, 298 (1964).
(9) R. Kubo, "Statistical Mechanics", North-Holland Publishing Co., Amsterdam, 1965, p 77.
(10) B. Van der Pol and H. Bremmer, "Operational Calculus Based on the Two-Sided Laplace Integral", Cambridge University Press, New York, N.Y., 1950.
(11) R. K. Wehner and D. Baeriswyl, *Physica A: (Amsterdam)*, **81A**, 129 (1975).
(12) S. Chandresekhar, *Rev. Mod. Phys.*, **15**, 1 (1943).
(13) Cf. section III of J. L. Doob, *Ann. Math. Stat.*, **43**, 351 (1942).
(14) A. Ralston and H. S. Wilf, Ed. "Mathematical Methods for Digital Computers", Part I, Wiley, New York, N.Y., 1963, Chapter 8.
(15) E. Helfand, *J. Chem. Phys.*, **54**, 4651 (1971).
(16) H. A. Kramers, *Physica (Utrecht)*, **7**, 284 (1940).
(17) Superposed bars denote dimensional quantities; corresponding dimensionless quantities, to be defined shortly, have bars omitted.
(18) Most of the computations reported on utilized $\eta = 0.1$ except for one case (Figure 9) where $\eta = 0.01$. In general it was noted that the value of η in this range ($0.01 \leq \eta \leq 0.1$) had little effect on the results of the type of computations performed here.